

Probing Li-Haldane conjecture with a perturbed boundary

Zenan Liu,¹ Rui-Zhen Huang,^{2,*} Zheng Yan,^{3,4,5,6,†} and Dao-Xin Yao^{1,7,‡}

¹*State Key Laboratory of Optoelectronic Materials and Technologies,
Guangdong Provincial Key Laboratory of Magnetoelectric Physics and Devices,
Center for Neutron Science and Technology, School of Physics,
Sun Yat-Sen University, Guangzhou 510275, China*

²*Department of Physics and Astronomy, Ghent University, Krijgslaan 281, S9, B-9000 Ghent, Belgium*

³*Department of Physics, School of Science, Westlake University,
600 Duncun Road, Hangzhou 310030, Zhejiang Province, China*

⁴*Institute of Natural Sciences, Westlake Institute for Advanced Study,
18 Shilongshan Road, Hangzhou 310024, Zhejiang Province, China*

⁵*Department of Physics and HKU-UCAS Joint Institute of Theoretical and Computational Physics,
The University of Hong Kong, Pokfulam Road, Hong Kong, China*

⁶*Lanzhou Center for Theoretical Physics & Key Laboratory of Theoretical Physics of Gansu Province,
Lanzhou University, Lanzhou, Gansu 730000, China*

⁷*International Quantum Academy, Shenzhen 518048, China*

(Dated: March 3, 2023)

The famous Li-Haldane conjecture relates the energy and bi-partite entanglement spectrum in many topological phases. This correspondence is usually satisfied in chiral ordered states or systems with a symmetry-protected gapless boundary. Although a lot of theoretical and numerical works have confirmed the conjecture in topological states with bulk-boundary correspondence, the cases with gapped boundary are widely unknown. Via newly developed quantum Monte Carlo (QMC) scheme, we extract the large-scale entanglement spectrum and study its relation with energy spectrum in the Affleck-Kennedy-Lieb-Tasaki (AKLT) phase with a tunable boundary on the square-octagon lattice. We find the low-lying entanglement spectrum does not always show similar behaviors as the energy spectrum on the tunable boundary. The breakdown of the correspondence originates from the perturbation in the environment and the coupling between the subsystem and its environment. This can be understood by the wormhole effect in the path integral representation of reduced density matrix. Our study generalizes the established correspondence between gapless/gapped boundary energy spectrum and entanglement spectrum, and further demonstrates there exists a deep connection between physical and entanglement degrees of freedom in quantum many-body systems.

INTRODUCTION

In the past decades, entanglement has become a key concept in describing quantum matters, especially exotic new quantum phases from the quantum information viewpoint. It leads to a unified understanding of quantum matter and information and serves as a quintessential quantity to detect and characterize the informational, field-theoretical, and topological properties of quantum many-body states [1–4], which combines the conformal field theory (CFT) and the categorical description of the problem [5–17]. For instance, bipartite entanglement entropy (EE) was widely used to identify quantum phases and phase transitions. The EE of the ground states usually satisfies an area law for locally interacting gapped systems. For topologically ordered systems, a topological EE term was also proposed to detect the quantum dimension of the topological excitation. It can also be used to detect conformal anomaly in even space-time dimensional theories.

More interestingly, the entanglement spectrum (ES) contains more information than EE [18]. The low-lying ES have been widely employed as a fingerprint of CFT and topology in the investigation of highly entangled

quantum matter [19–36]. For a critical theory with conformal symmetry in one space dimension, the entanglement Hamiltonian of a subsystem in the ground state corresponding to a boundary CFT and the low-lying ES can be used to detect operator contents [37, 38]. For topologically ordered phases with gapless boundaries, the famous Li-Haldane conjecture relates the low-lying ES to the energy spectrum [18]. They demonstrated that the general $\nu = 5/2$ topological states have the same low-lying ES to identify the topology and CFT structure on the boundary.

Numerical results have also shown that the relation between the low-lying ES and boundary energy spectrum exists generally in some magnetic systems beyond topological states [19, 39, 40]. Then, it was theoretically shown to be a general relationship between the entanglement spectrum of (2+1)d chiral gapped topological states and the energy spectrum on their (1+1)d edges [22]. Following studies [41–47] also confirm this conjecture. However, there is generally no correspondence between the low energy spectrum of edge Hamiltonian and entanglement Hamiltonian in the non-chiral topological phase without symmetry enrichment [48], in which the boundary can be gapped. A deep understanding for the break-

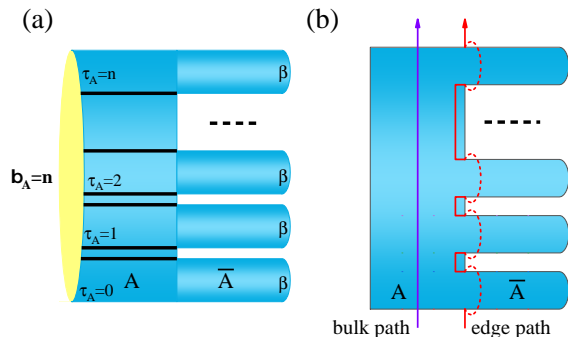


FIG. 1. (a) A geometrical structure of the partition function $\mathcal{Z}_A^{(n)}$. The subsystem A is entangled with the environment \bar{A} . Each replica connects with each other in A , while the environment \bar{A} for each replica is independent. $\beta_A = n$ represents the imaginary-time length in A and β is $1/T$ for total system. (b) A schematic picture of worldlines crossing a replica. The subsystem A is coupled with the environment \bar{A} via J_y . These worldlines which cross the bulk will decay to zero as $\beta \rightarrow \infty$ in principle. Meanwhile, the ones which cross the imaginary-time edge of \bar{A} will arrive at the next replica without much cost.

down of correspondence between the entanglement and physical boundary spectrum is still lacking.

To probe the Li-Haldane conjecture in a more general setting, we numerically study the entanglement properties of a two-dimensional AKLT model, perturbed by a small symmetry-breaking interaction on the boundary. The AKLT phase is protected by the global spin rotation symmetry and translation invariance, whose physical and entanglement boundary are both expected to be gapless under the symmetry constraint. For the topological phase, when the perturbation is added to the boundary, our results may become inconsistent with the Li-Haldane conjecture. To systematically explore the reasons for the possible inconsistency of the correspondence between the physical and entanglement boundary spectrum, we tune the coupling between the subsystem and environment. The coupling serves as a key role to change the entanglement boundary dramatically by transporting the interaction of the environment. It can be naturally understood through the wormhole effect in the path integral picture of the reduced density matrix [40], as depicted in Fig. 1, which will be explained in the following section. The coupling between the subsystem and environment makes the imaginary path length of imaginary time near the entangled boundary much shorter than that in the bulk, which makes the perturbation near the entanglement boundary in the environment important. As a result, the entanglement spectrum on the boundary may become different from the physical boundary energy spectrum, which is inconsistent with the Li-Haldane conjecture. These interesting results inspire the general relation between the ES and energy spectrum and call for new physics beyond

the Li-Haldane conjecture.

MODEL AND METHOD

We investigate the $S = 1/2$ Heisenberg model on the square-octagon lattice with C_{4v} lattice symmetry, whose Hamiltonian in the bulk can be written as

$$H_b = J_1 \sum_{\langle ij \rangle} \mathbf{S}_i \cdot \mathbf{S}_j + J_2 \sum_{\langle ij \rangle'} \mathbf{S}_i \cdot \mathbf{S}_j \quad (1)$$

where the inter-unit-cell coupling $J_1 = 1$ as the unit energy scale and intra-unit-cell coupling $J_2 > 0$. The model hosts a rich phase diagram for the ground states under the competition between J_1 and J_2 terms. There are four phases including $S = 2$ Néel phase, AKLT phase, $S = 1/2$ Néel phase and plaquette valence bond crystal (PVBC), which are separated by three $O(3)$ quantum critical points [49]. The AKLT state is a symmetry protected topological (SPT) state and has gapless boundaries protected by the translation invariance and spin rotation symmetry. The gapless boundary can be modeled by an effective $S = 1/2$ Heisenberg chain [50]. Surprisingly, the influence of the gapless boundary even extends the physics of $O(3)$ critical point and induces unconventional surface critical behaviors [49]. To investigate the Li-Haldane conjecture deeply, i.e., the relation between the physical and entanglement boundary modes, we add other terms to the original Hamiltonian

$$H = H_b + J_s \sum_{\langle ij \rangle_s} \mathbf{S}_i \cdot \mathbf{S}_j + J_y \sum_{\langle ij \rangle_y} \mathbf{S}_i \cdot \mathbf{S}_j \quad (2)$$

where J_s is a small translation-invariance-breaking term on the boundary and J_y is the coupling between the subsystem A and environment \bar{A} which can change the boundary condition along the y direction. Fig. 2 depicts the model Eq. 2 on the square-octagon lattice.

We use the recently proposed QMC-based numerical method to study the low-lying ES [40]. In the framework of QMC, it is difficult to construct the $\rho_A = \text{Tr}_{\bar{A}}(|\psi\rangle\langle\psi|)$ directly as exact diagonalization [39] and density matrix renormalization group do [45, 46]. The ES can be obtained through stochastic analytic continuation (SAC) from the imaginary-time evolution of ρ_A in the QMC simulations [51–53]. Specifically, by introducing an effective imaginary time n for the entanglement Hamiltonian, the effective partition function can be written as

$$\mathcal{Z}_A^{(n)} = \text{Tr}[\rho_A^n] = \text{Tr}[e^{-n\mathcal{H}_A}] \quad (3)$$

where the effective imaginary time $\beta_A = n$. By constructing the modified manifold in the QMC simulations (Fig. 1), we can obtain the imaginary-time spin correlation $G(\tau_A, \mathbf{q}) = \langle S_{-\mathbf{q}}^z(\tau_A) S_{\mathbf{q}}^z(0) \rangle$ for the entanglement Hamiltonian \mathcal{H}_A and then find the corresponding ES in

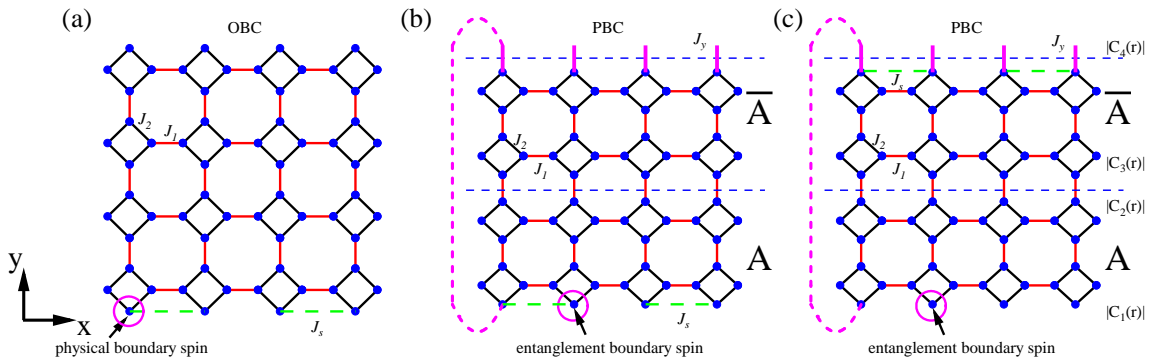


FIG. 2. Schematic figures of the model Eq. 2 on the square-octagon lattice under periodic boundary condition (PBC) along the x direction and a tunable boundary in the y direction. (a) Open boundary condition (OBC) in the y direction and J_s perturbations at the lower edge. (b-c) A tunable boundary coupling \overline{J}_y along the y direction and J_s perturbations at the entanglement boundary which is marked by blue dashed lines. A and \overline{A} denote the subsystem and environment respectively. The J_y coupling can change boundary conditions along the y direction. In particular, the system is under PBC or OBC when $J_y = 1$ or $J_y = 0$ respectively.

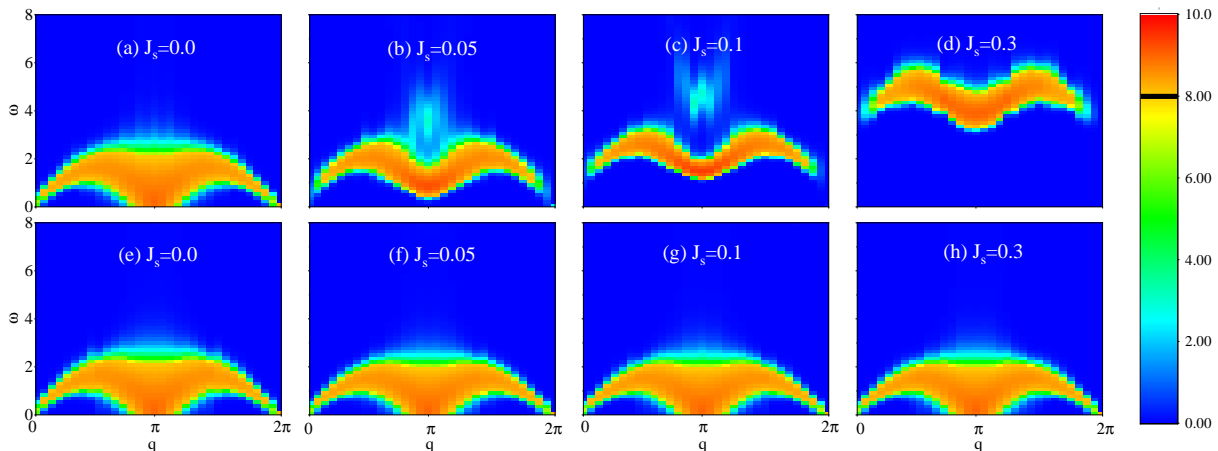


FIG. 3. Dynamical spectra for the $J_1 - J_2$ Heisenberg model on the square-octagon lattice under a modified boundary as in Fig. 2(a) with $L = 32$ and $\beta = 64$. Upper panel: Dynamical spectra on the bottom boundary. Lower panel: Dynamical spectra on the top boundary. For better presentation, we set the color bars to be logarithmic scale above 8.0.

the spectral function $G(\omega_0, \mathbf{q})$ via SAC, where ω_0 is the original frequency. Due to the lack of a natural energy scale in the entanglement Hamiltonian, it is difficult to compare the ES in systems with different parameters. To resolve this problem, we have normalized the ES with the bandwidth and denoted the spectral function as $G(\omega, \mathbf{q})$.

An interesting wormhole effect inducing the low-lying ES has been put forward recently [40]. In the replica manifold structure as Fig. 1 (b) shows, because the trace of environment glues the upper and nether boundaries of one replica, it provides a convenient way for worldlines to teleport from bottom to top, which makes the path length of imaginary time near the entangled edge path (red line of Fig. 1 (b)) is much shorter than in the bulk (blue line of Fig. 1 (b)). According to the path integral in which the shorter path length provides larger weight, the edge mode plays an important role in the low-lying

ES. Thus the Li-Haldane conjecture has been explained well within the wormhole mechanism.

In this work, we concentrate on the AKLT state of the model (Eq. 2) in the bulk with the system size $L = 32$ and $J_2 = 0.3$. The bulk has a large energy gap, where the low energy physics is governed by its boundary. In addition, due to the spin rotation symmetry of the model, we can only consider the imaginary-time boundary correlation for the s^z operator, $G(\tau_A, \mathbf{q}) = \frac{1}{L} \sum_{i,j} e^{-i\mathbf{q}\cdot(\mathbf{x}_i - \mathbf{x}_j)} \langle s_i^z(\tau) s_j^z(0) \rangle$, where s_i^z denotes spins on the physical or entanglement boundary.

RESULTS

In this section, we first study the influence of the small perturbation term J_s to the ES with a full cou-

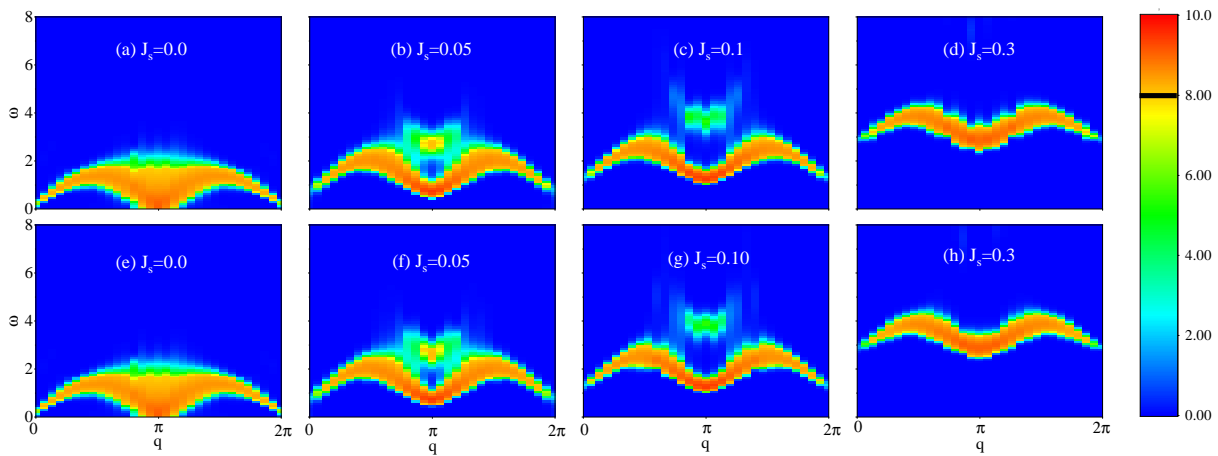


FIG. 4. Entanglement spectra for the $J_1 - J_2$ Heisenberg model on the square-octagon lattice under a modified entanglement boundary as in Fig.2 (b) and (c). Upper panel: Entanglement spectra of the bottom edge as shown in Fig.2 (b). Lower panel: Entanglement spectra of the bottom edge as shown in Fig.2 (c). For better presentation, we set the color bars to be logarithmic scale above 8.0.

pling strength J_y , i.e., under the periodic boundary condition (PBC) in the y direction. Then we tune the coupling J_y to systematically explore how the correspondence between the boundary ES and energy spectrum breaks down, including the case of $J_y = 0$ i.e. the case of open boundary condition (OBC).

Probing the Li-Haldane conjecture with perturbed boundaries.- As Fig. 2 illustrates, when the boundary is gapped by the perturbation, we make a comparison study between low-lying spectra on the physical and entanglement boundaries, i.e., the energy spectra on the physical boundary for a system under OBC and entanglement spectra on the entanglement boundary for a system under PBC ($J_y = 1$).

The energy spectra are presented in Fig. 3 through the boundary spin-spin dynamical spectral function. Without the translation-invariance-breaking term, $J_s = 0$, two physical boundaries are both gapless and can be modeled by a one-dimensional spin-1/2 Heisenberg model. The spin-spin dynamical spectral function corresponds to the two-spinon excitation, which is consistent with the feature of gapless boundary of SPT phases. Without symmetry protection, the boundary is not guaranteed to be gapless. As shown in Fig. 3 (a-d), when J_s increases, the perturbed boundary becomes gapped in which the excitation becomes magnon and the energy gap is larger for stronger J_s . Meanwhile, the other untouched boundary remains gapless, see Fig. 3 (e-f).

Interestingly, for the entanglement boundary, we find the entanglement spectrum in Fig. 4 does not always show similar features as the energy spectrum of subsystem A as an independent physical system under OBC. Without the perturbation term, $J_s = 0$, the entanglement boundary is gapless as demonstrated in Fig. 4(a) and (e), which is consistent with the Li-Haldane con-

jecture. With a small J_s term on the entanglement boundary, the entanglement spectrum on the lower boundary of A becomes gapped whether we put J_s in A or \bar{A} as shown in Fig. 3 (b-d) and (f-h) respectively. For the former case (J_s in the subsystem A), the Li-Haldane conjecture applies well. Both physical and entanglement boundaries are gapped. While for the latter case (J_s in the environment \bar{A}), the entanglement spectrum on the lower boundary of A does not follow the gapless physical boundary of A as an independent system under OBC. This means a symmetry breaking perturbation in the environment can change the entanglement spectrum dramatically. Besides, if we gap the lower edge of A and the upper edge of \bar{A} via the perturbation J_s near the entanglement boundary, the ES gap becomes twice as large as the case that only one boundary is gapped (see Appendix C). So the environment and subsystem hold the same position in the ES.

These results demonstrate that interactions in the environment can change the entanglement Hamiltonian of the subsystem A through the coupling J_y connecting the subsystem and environment. Actually, according to the path-integral picture for the entanglement Hamiltonian, this change can be understood naturally as the so-called wormhole effect [40]. As shown in Fig.1 (b), the red line path near the entangled edge is the shortest path to contribute to the low-lying ES. Under the PBC, or with a full strength coupling $J_y = 1$, the path goes through the edges of both A and \bar{A} alternately, thus the perturbation on the lower boundary of A or upper boundary of \bar{A} plays a similar role in the path-integral and both of them results in the gapped boundary ES.

The role of the coupling between system and environment.- To further explore the influence of wormhole effect on the correspondence between energy and

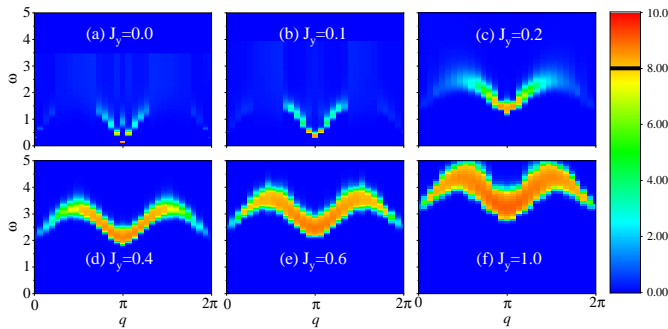


FIG. 5. The rescaled entanglement spectra of Fig.2 (c) with $J_s = 0.3$, $\beta = 50$ and $\beta_n = 64$, where J_y is (a)-(f) 0.0, 0.1, 0.2, 0.4, 0.6, and 1.0. For better presentation, we set the color bars to be logarithmic scale above 8.0.

entanglement spectrum, we systematically study the ES with different coupling strength J_y between the subsystem and environment.

Firstly our analysis in the last section can be directly examined by turning off J_y . In this case, the whole system is under OBC in the y direction and the subsystem A has one physical boundary and entanglement boundary. When putting the symmetry breaking perturbation J_s in \bar{A} (upper boundary), the entanglement spectrum on the lower boundary of A should follow the Li-Haldane conjecture now, as there is no coupling between subsystem and environment ($J_y = 0$) and no wormhole effect. Our numerical results also confirm the analysis as Fig. 5 (a) illustrates. Without the coupling connecting the subsystem and environment, the Li-Haldane conjecture is always satisfied on this open boundary.

For general cases, the coupling J_y serves as a medium that transports the perturbation in the environment to the entanglement spectrum on the boundary of subsystem A . It is expected that such an effect would be turned on and amplified when J_y is increased from $J_y = 0$ gradually to its full strength $J_y = 1$. As shown in Fig. 5 (b-f), the entanglement spectrum gap is opened and becomes larger as J_y increases, which again supports our analysis. In the appendix we also discuss the spectral function $G(\omega_0, \mathbf{q})$ without a normalization. In fact, the coupling can increase the wormhole effect which makes the environment gap hold the main position. And the interplay between the coupling and perturbation demonstrates that the ES can be controlled via the wormhole effect (see Appendix). Other more general settings are presented in the appendix, which are all consistent with the analysis here.

These numerical results together with the qualitative analysis from the path-integral picture indicate that the entanglement spectrum on the boundary of gapped phases can be changed via the modification of the environment and the coupling between the subsystem and environment. This analysis reveals that the coupling can

be considered as a mechanism for the inconsistency of the correspondence between energy and entanglement spectrum.

DISCUSSION

In the original Li-Haldane conjecture, the coupling strength between subsystem and environment was not explored. It is usually limited to special systems that have SPT order or chiral topological order. It has been shown that such a correspondence may not hold in the non-chiral topological ordered states. There is no general physical picture to explain it. Our study here reveals that an important missing point is the role of coupling between the subsystem and its environment. From the path integral picture for the partition function in the replica manifold (Fig. 2), it is clear that the coupling makes the boundary of A and \bar{A} contributes much more importantly than the bulk. The worldlines near the entanglement boundary cross the edge of A and \bar{A} alternately so that both boundary perturbations of A and \bar{A} contribute to the low-lying ES. This path-integral on replica manifold provides a simple picture and mechanism for the inconsistency of correspondence between the energy and entanglement spectrum on the boundary.

In this work, we limited our study near the boundaries for a gapped SPT phase and symmetric couplings J_y between the subsystem and its environment. It is not clear how the entanglement spectrum be changed by perturbations and couplings in general cases. It would be still natural that the coupling between the system and environment also serves as a key role. Without the coupling between the subsystem and its environment, local perturbations in the environment have large imaginary time in the replica manifold and can not contribute a lot to the ES. Although we only concentrated on one boundary, these analyses also apply to the other unperturbed boundary, i.e. the upper or lower boundary of A or \bar{A} respectively. The importance of the coupling between the subsystem and its environment in the Li-Haldane conjecture also reflects the quantum nature of entanglement. Without any coupling, the whole system becomes a tensor product of A and \bar{A} and there would be no entanglement at all. And for no coupling, the entanglement boundary of subsystem A can be naturally described by an effective $S = 1/2$ Heisenberg chain (see Appendix D).

When the bulk is a critical point or gapless phase, it is still not clear whether the Li-Haldane conjecture applies. For those critical theories which can be described by a conformal field theory in one space dimension, it seems the conjecture also applies [37]. Studies here may also be carried out to analyze the correspondence, especially for those symmetry-enriched critical points [36, 54].

CONCLUSION

In summary, we have systematically studied the relation between the energy and entanglement spectrum on the boundary in the AKLT phase of the $S = 1/2$ Heisenberg model on the square-octagon lattice with a symmetry-breaking term on the boundary and a tunable coupling between the subsystem and its environment. The correspondence does not always apply if the perturbation is added to the environment. The entanglement spectrum can show different behaviors as the energy spectrum of the subsystem as an independent system under open boundary condition. Tuning the coupling between the subsystem and environment can change the ES gap, which indicates that the coupling accounts for the inconsistency of the Li-Haldane conjecture. This inconsistency can be naturally explained in the path integral representation for the partition function in the replica manifold. In the path-integral picture, the wormhole effect induced by the coupling plays an important role in transporting the interaction of the environment and provides a pathway to control the ES. The rapidly developed quantum circuits experiments have successfully extracted the ES through measuring different orders of Rényi entropies [55–58]. The basic idea is to fit the low-lying ES according to the $1 \sim n$ order Rényi entropies [15], where the n is a cut-off order. Besides, the recent cold atom experiment has successfully probed the Li-Haldane conjecture in the topological states by using entanglement Hamiltonian tomography and quantum variational learning [59]. It makes the possibility that our results can be realized in the quantum circuits and cold atom systems via constructing and controlling the AKLT or other SPT states.

ACKNOWLEDGEMENTS

Z.Y. would like to thank Bin-Bin Chen, Shangqiang Ning and Zi Yang Meng for fruitful discussions. Z.L. and D.X.Y. are supported by NKRDPC-2022YFA1402802, NKRDPC-2018YFA0306001, NSFC-11974432, NSFC-92165204, GBABRF-2019A1515011048, Leading Talent Program of Guangdong Special Projects (201626003), and Shenzhen International Quantum Academy (Grant No. SIQA202102). The authors also acknowledge Beijing PARATERA Tech Co.,Ltd.(<https://www.paratera.com/>) for providing HPC resources that have contributed to the research results reported within this paper. R.Z.H. is supported by a postdoctoral fellowship from Ghent university - Special Research Fund (BOF). Z.Y. thanks the support from the open fund of Lanzhou Center for Theoretical Physics (12247101).

- * ruizhen.huang@ugent.be
 † zhengyan@westlake.edu.cn
 ‡ yaodaax@mail.sysu.edu.cn
- [1] G. Vidal, J. I. Latorre, E. Rico, and A. Kitaev, *Phys. Rev. Lett.* **90**, 227902 (2003).
 - [2] V. E. Korepin, *Phys. Rev. Lett.* **92**, 096402 (2004).
 - [3] A. Kitaev and J. Preskill, *Phys. Rev. Lett.* **96**, 110404 (2006).
 - [4] M. Levin and X.-G. Wen, *Phys. Rev. Lett.* **96**, 110405 (2006).
 - [5] P. Calabrese and A. Lefevre, *Phys. Rev. A* **78**, 032329 (2008).
 - [6] E. Fradkin and J. E. Moore, *Phys. Rev. Lett.* **97**, 050404 (2006).
 - [7] Z. Nussinov and G. Ortiz, *Proc. Nat. Acad. Sci.* **106**, 16944 (2009).
 - [8] Z. Nussinov and G. Ortiz, *Annals Phys.* **324**, 977 (2009).
 - [9] H. Casini and M. Huerta, *Nuclear Physics B* **764**, 183 (2007).
 - [10] W. Ji and X.-G. Wen, *Phys. Rev. Research* **1**, 033054 (2019).
 - [11] W. Ji and X.-G. Wen, *Phys. Rev. Research* **2**, 033417 (2020).
 - [12] L. Kong, T. Lan, X.-G. Wen, Z.-H. Zhang, and H. Zheng, *Phys. Rev. Research* **2**, 043086 (2020).
 - [13] X.-C. Wu, W. Ji, and C. Xu, *Journal of Statistical Mechanics: Theory and Experiment* **2021**, 073101 (2021).
 - [14] X.-C. Wu, C.-M. Jian, and C. Xu, *SciPost Phys.* **11**, 33 (2021).
 - [15] J. Zhao, Y.-C. Wang, Z. Yan, M. Cheng, and Z. Y. Meng, *Phys. Rev. Lett.* **128**, 010601 (2022).
 - [16] J. Zhao, B.-B. Chen, Y.-C. Wang, Z. Yan, M. Cheng, and Z. Y. Meng, *npj Quantum Materials* **7**, 1 (2022).
 - [17] Y.-C. Wang, N. Ma, M. Cheng, and Z. Y. Meng, *arXiv e-prints*, arXiv:2106.01380 (2021), arXiv:2106.01380 [cond-mat.str-el].
 - [18] H. Li and F. D. M. Haldane, *Phys. Rev. Lett.* **101**, 010504 (2008).
 - [19] F. Pollmann, A. M. Turner, E. Berg, and M. Oshikawa, *Phys. Rev. B* **81**, 064439 (2010).
 - [20] L. Fidkowski, *Phys. Rev. Lett.* **104**, 130502 (2010).
 - [21] H. Yao and X.-L. Qi, *Phys. Rev. Lett.* **105**, 080501 (2010).
 - [22] X.-L. Qi, H. Katsura, and A. W. W. Ludwig, *Phys. Rev. Lett.* **108**, 196402 (2012).
 - [23] E. Canovi, E. Ercolessi, P. Naldesi, L. Taddia, and D. Vodola, *Phys. Rev. B* **89**, 104303 (2014).
 - [24] D. J. Luitz, F. Alet, and N. Laflorencie, *Phys. Rev. Lett.* **112**, 057203 (2014).
 - [25] D. J. Luitz, F. Alet, and N. Laflorencie, *Phys. Rev. B* **89**, 165106 (2014).
 - [26] D. J. Luitz, N. Laflorencie, and F. Alet, *Journal of Statistical Mechanics: Theory and Experiment* **2014**, P08007 (2014).
 - [27] C.-M. Chung, L. Bonnes, P. Chen, and A. M. Läuchli, *Phys. Rev. B* **89**, 195147 (2014).
 - [28] H. Pichler, G. Zhu, A. Seif, P. Zoller, and M. Hafezi, *Phys. Rev. X* **6**, 041033 (2016).
 - [29] J. I. Cirac, D. Poilblanc, N. Schuch, and F. Verstraete, *Phys. Rev. B* **83**, 245134 (2011).
 - [30] V. M. Stojanović, *Phys. Rev. B* **101**, 134301 (2020).

- [31] W.-z. Guo, Journal of High Energy Physics **2021**, 1 (2021).
- [32] T. Grover, Phys. Rev. Lett. **111**, 130402 (2013).
- [33] F. F. Assaad, T. C. Lang, and F. Parisen Toldin, Phys. Rev. B **89**, 125121 (2014).
- [34] F. F. Assaad, Phys. Rev. B **91**, 125146 (2015).
- [35] F. Parisen Toldin and F. F. Assaad, Phys. Rev. Lett. **121**, 200602 (2018).
- [36] X.-J. Yu, R.-Z. Huang, H.-H. Song, L. Xu, C. Ding, and L. Zhang, Phys. Rev. Lett. **129**, 210601 (2022).
- [37] A. M. Läuchli, arXiv preprint arXiv:1303.0741 (2013).
- [38] J. Cardy and E. Tonni, Journal of Statistical Mechanics: Theory and Experiment **2016**, 123103 (2016).
- [39] D. Poilblanc, Phys. Rev. Lett. **105**, 077202 (2010).
- [40] Z. Yan and Z. Y. Meng, “Relating entanglement spectra and energy spectra via path-integral on replica manifold,” (2021).
- [41] W. Zhu, Z. Huang, Y.-C. He, and X. Wen, Phys. Rev. Lett. **124**, 100605 (2020).
- [42] W. Zhu, Z. Huang, and Y.-C. He, Phys. Rev. B **99**, 235109 (2019).
- [43] Q.-C. Tang and W. Zhu, Chinese Physics Letters **37**, 010301 (2020).
- [44] W.-J. Rao, X. Wan, and G.-M. Zhang, Phys. Rev. B **90**, 075151 (2014).
- [45] J. I. Cirac, D. Poilblanc, N. Schuch, and F. Verstraete, Phys. Rev. B **83**, 245134 (2011).
- [46] Y.-C. He, D. N. Sheng, and Y. Chen, Phys. Rev. Lett. **112**, 137202 (2014).
- [47] C. Fang, M. J. Gilbert, and B. A. Bernevig, Phys. Rev. B **87**, 035119 (2013).
- [48] W. W. Ho, L. Cincio, H. Moradi, D. Gaiotto, and G. Vidal, Phys. Rev. B **91**, 125119 (2015).
- [49] L. Zhang and F. Wang, Phys. Rev. Lett. **118**, 087201 (2017).
- [50] Z. Liu, J. Li, R.-Z. Huang, J. Li, Z. Yan, and D.-X. Yao, Phys. Rev. B **105**, 014418 (2022).
- [51] A. W. Sandvik, Phys. Rev. E **94**, 063308 (2016).
- [52] H. Shao, Y. Q. Qin, S. Capponi, S. Chesi, Z. Y. Meng, and A. W. Sandvik, Phys. Rev. X **7**, 041072 (2017).
- [53] H. Shao and A. W. Sandvik, Physics Reports **1003**, 1 (2023).
- [54] R. Verresen, R. Thorngren, N. G. Jones, and F. Pollmann, Physical Review X **11**, 041059 (2021).
- [55] S. Johri, D. S. Steiger, and M. Troyer, Phys. Rev. B **96**, 195136 (2017).
- [56] P.-Y. Chang, X. Chen, S. Gopalakrishnan, and J. H. Pixley, Phys. Rev. Lett. **123**, 190602 (2019).
- [57] L. Zhang, J. A. Reyes, S. Kourtis, C. Chamon, E. R. Mucciolo, and A. E. Ruckenstein, Phys. Rev. B **101**, 235104 (2020).
- [58] A. Lavasani, Y. Alavirad, and M. Barkeshli, Nature Physics **17**, 342 (2021).
- [59] T. V. Zache, C. Kokail, B. Sundar, and P. Zoller, Quantum **6**, 702 (2022).

Appendix A: Different coupling strength with $J_s = 0.0$

In this section, we tune J_y from 0 to 1.0 with $\beta = 50$ and $\beta_A = 64$ to explore the wormhole effect on ES without normalization. The wormhole effect can lower the edge modes which is clearly shown in the original ES with $J_s = 0.0$ in Fig.6. Because $\Delta\tau = 1$ for replica structure is too large to obtain the high-energy part on ES by SAC, we only observe the low-energy excitation in Fig.6 (a) and (b), which is enough to analyse the important entanglement message. At $J_y = 0$ limit, the edge becomes a real physical edge and the ES has a small gap. Although the ES should become gapless two spinon continuum in the AKLT phase, the finite size gap becomes larger in ES because the wormhole effect disappears at $J_y = 0$. The gap is amplified β times due to the replica system. This amplification effect leads to the ES gap.

Then, the gap of ES becomes smaller and smaller when J_y increases, which demonstrates that the wormhole effect is magnified as J_y increases. Thus, the wormhole effect makes the ES gap become smaller as J_y increases, which lowers the bulk amplification effect and makes the bandwidth become smaller at the same time. Actually, the gap change can not be derived directly from the original Li-Haldane conjecture. The coupling strength plays an important role in the ES mechanism which has been confirmed in our numerical results.

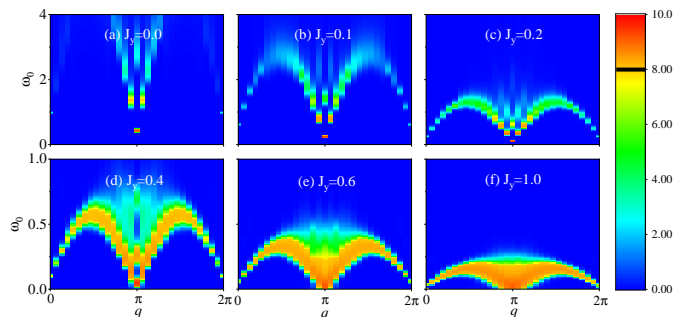


FIG. 6. The original entanglement spectra of Fig.2 (c) with $J_s = 0.0$, $\beta = 50$ and $\beta_n = 64$, where J_y is (a)-(f) 0.0, 0.1, 0.2, 0.4, 0.6, and 1.0. For better presentation, we set the color bars to be logarithmic scale above 8.0.

Appendix B: Different coupling strength with $J_s = 0.3$

The original entanglement spectra without rescaling are presented here to understand the competition between wormhole effect and the coupling strength from the replica picture with $J_s = 0.3$. The inverse temperature β is 50 and β_A is 64. When J_y is from 0 to 0.2, the ES gap gradually becomes large. And then the gap gets smaller

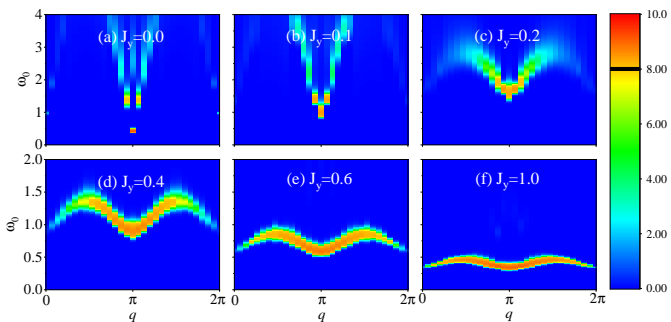


FIG. 7. The original entanglement spectra of Fig.2 (c) with $J_s = 0.3$, $\beta = 50$ and $\beta_n = 64$, where J_y is (a)-(f) 0.0, 0.1, 0.2, 0.4, 0.6, and 1.0. For better presentation, we set the color bars to be logarithmic scale above 8.0.

and smaller with increasing the coupling strength as Fig.7 shows. The gap change looks non-monotonous which is different from the $J_s = 0$ case. The environment edge becomes gapped at $J_s = 0.3$ which will make the ES much gapped as J_y increases. But the wormhole effect can be magnified by increasing the coupling strength J_y . These competing reasons lead to the non-monotonous behavior of gap change in the ES. At small J_y , the environment gap dominantly contributes to the ES gap because of the weaker wormhole effect. Thus, the ES gap becomes large with increasing J_y . The wormhole effect can hold the dominant position when J_y is enough large, which makes the ES gap becomes smaller as we continue increasing the coupling to the full strength $J_y = 1$. So the perturbation J_s on the environment can make the ES gapped at the lower boundary of A via the coupling, which is different from the gapless boundary of A and inconsistent with the Li-Haldane conjecture.

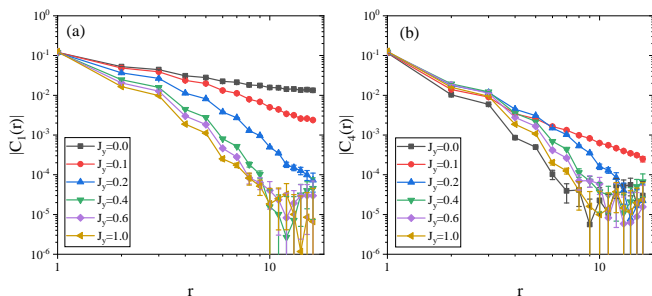


FIG. 8. Boundary equal-time correlation functions of Fig.2 (c) at $J_s = 0.3$. (a) The correlation functions $|C_1(r)|$ for the lower boundary of subsystem A with different J_y . (b) The correlation functions $|C_2(r)|$ for the upper boundary of subsystem \bar{A} with different J_y .

We notice that, for the equal-time spin correlation functions, as J_y increases, both $|C_1(r)|$ and $|C_4(r)|$ decay faster and faster. If we think the gap is in direct proportion to the velocity of correlations, it seems similar to the $J_s = 0.0$ case. Therefore, in this view, the entanglement

Hamiltonian gap also becomes larger and larger, but it is contradictory to the gap change in the original ES due to the different energy scale in the entanglement Hamiltonian. Actually, to rescale the original ES by the bandwidth of ES. As Fig.5 illustrates, the rescaling ES gap becomes larger and larger when increasing the coupling strength, which is consistent with the cases in the equal-time correlations. Therefore, the bandwidth can represent the energy scale of entanglement Hamiltonian in some special cases.

Appendix C: More boundary interactions

If more boundary interactions are tuned near the entanglement edge, it is unclear whether the ES will be like the edge spectrum. We focus on the energy spectrum and entanglement spectrum of Fig.9, where the perturbation J_s is added to two boundaries with $J_y = 1$. When $J_s = 0.3$, the edge spectrum of the model becomes gapped excitation (Fig.10 (a)) which is similar to Fig.3 (d). If the perturbation J_s is added to the bottom edge of subsystem and top edge of environment to gap them at the same time (Fig.9 (b)), the ES becomes also gapped (Fig.10 (b)). And its gap is nearly twice as large as the ES at Fig.10 (c-d), which demonstrates that both subsystem and environment perturbation contribute to the ES equally. It further proves that the coupling J_y can transport the environment perturbation to the subsystem near the entanglement boundary. Furthermore, we simulate the ES with $J_s = 0.3$ on the lower and upper boundaries of environment \bar{A} . In our expectation, the ES are also gapped on both boundaries of subsystem A as Fig.10(c) and (d) shows, which are similar to the energy spectrum.

Appendix D: boundary correlation function

In order to detect the feature of entanglement Hamiltonian, we obtain different sizes of the boundary equal-time correlation functions $|C_1(r)|$ and $|C_2(r)|$ in Fig.11, where $C_k(r) = \langle S_i^z S_j^z \rangle$ marked in Fig.2 (c). The system sizes in the simulation are from 16 to 40 with $\beta = 50$ and $\beta_n = 2L$. $|C_1(r)|$ represents the behaviors for entanglement boundary of A without coupling, while $|C_2(r)|$ shows the behaviors for the boundary of A with the full strength coupling. As shown in Fig.11 (3), it is clear that $|C_1(r)|$ and $|C_2(r)|$ decay in a power law which is consistent with the gapless boundary behaviors. This means that the bound of A without coupling is similar to the bound of A with full-strength coupling. After rescaling the correlation functions $C(r) = r^{-\eta} f(r/L)$ with $\eta = 1$, we show that $|C_1(r)|$ and $|C_2(r)|$ can almost collapse into a single curve. The exponent $\eta = 1$ is the anomalous dimension which is suitable for the (1+1)D gapless bound-

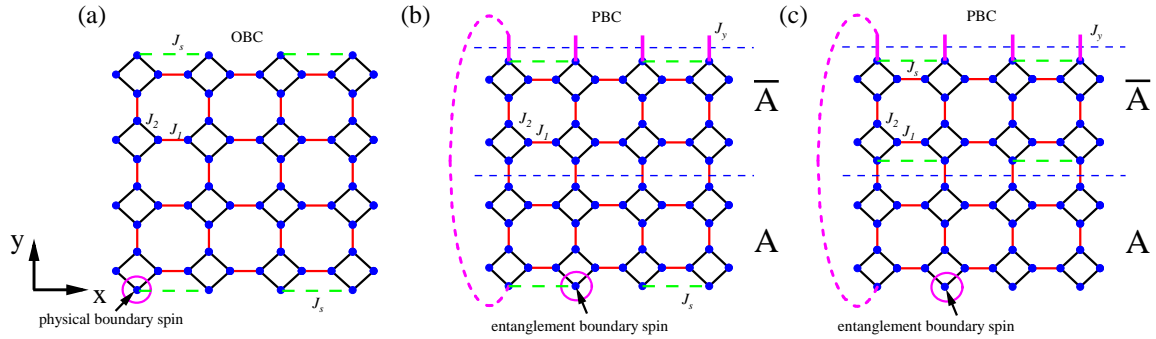


FIG. 9. The square-octagon lattice with the PBC in x direction. (a) The lattice with OBC in y direction with $J_y = 1$. (b) The lattice with PBC in y direction. The blue dashed line cut it into two entangled part, A and \bar{A} . And J_s is added to the lower boundary of subsystem A and upper boundary of \bar{A} as green dashed lines show. (c) The lattice with PBC in y direction, where J_s is added to the upper boundary and lower boundary of environment \bar{A} as green dashed lines show.

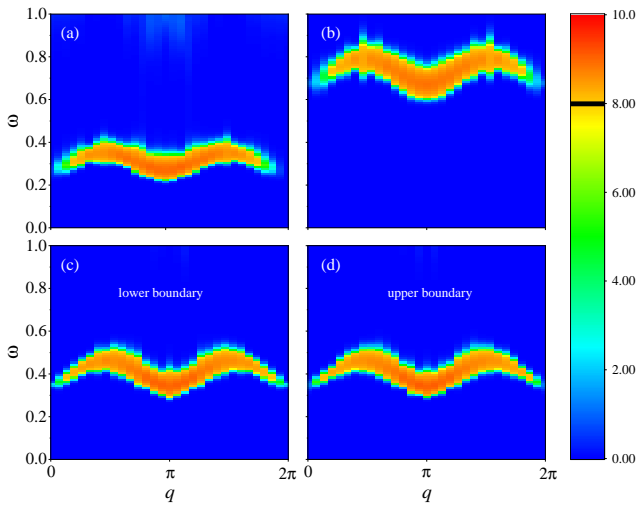


FIG. 10. The original dynamical spectra and entanglement spectra of Fig.9 with $J_y = 1$. (a) Dynamical spectrum with $J_s = 0.3$. (b) Entanglement spectrum of the lower boundary of subsystem A at Fig. 9 (b) with $J_s = 0.3$. (c) Entanglement spectrum of the lower boundary of subsystem A at Fig.9 (c) with $J_s = 0.3$. (d) Entanglement spectrum of the upper boundary of subsystem A at Fig.9 (c) with $J_s = 0.3$. For better presentation, we set the color bars to be logarithmic scale above 8.0.

ary of AKLT state, though there is a logarithm correction to the correlation function $C(r) \propto 1/r$ in a $S = 1/2$ Heisenberg chain. And the collapse picture clearly shows that $|C_1(r)|$ and $|C_2(r)|$ decay with the same power-law exponents, which indicates the entanglement Hamiltonian can be modeled by an effective $S = 1/2$ Heisenberg chain with and without coupling.

Appendix E: Finite size scaling

Although the ES gap is magnified β times, it should satisfy the finite size scaling of gap. Imaginary-time cor-

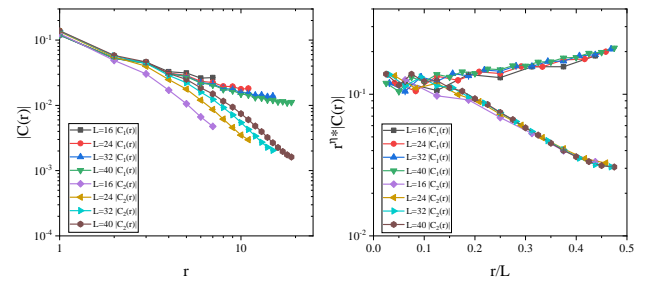


FIG. 11. Different lattice sizes L of boundary equal-time correlation functions $C_k(r)$ of Fig.2 (c) at $J_s = 0.3$ and $J_y = 0.0$. (a) The original boundary equal-time correlation $|C_1(r)|$ and $|C_2(r)|$ with $L=16, 24, 32$ and 40 . (b) Rescaling of $|C_1(r)|$ and $|C_2(r)|$ for different sizes L . The exponent $\eta = 1$ is the anomalous dimension.

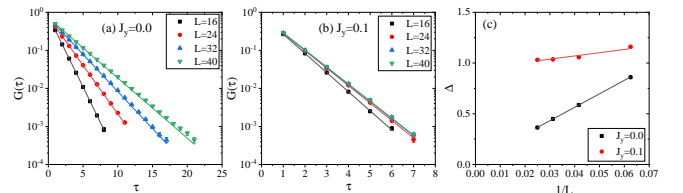


FIG. 12. The finite size scaling of entanglement spectra for Fig.2 (c) with $J_s = 0.3$, $\beta = 50$ and $\beta_n = 2L$. (a) Imaginary-time correlation function $G(\tau)$ at $q = \pi$ with $J_y = 0.0$. (b) Imaginary-time correlation function $G(\tau)$ at $q = \pi$ with $J_y = 0.1$. (c) Different sizes of entanglement spectra gap with $J_y = 0.0$ and $J_y = 0.1$.

relations $G(\tau)$ at $q = \pi$ are measured with $J_y = 0.0$ and $J_y = 0.1$ at $J_s = 0.3$, and we perform the finite-size scaling analysis of ES gap in Fig.12. In this calculation, the total system size is from 16 to 40. These gap values are obtained from the fitting of $G(\tau)$ that should satisfy $G(\tau) = be^{-\Delta\tau}$, where Δ refers to the gap. The ES gap should obey the finite-size scaling form $\Delta = \Delta(\infty) + bL^{-1}$, where b is the fitting parameters and $\Delta(\infty)$ is the ES gap in the thermodynamic limit.

As Fig.12 shows, it is clear that all $G(\tau)$ decay exponentially and are fitted well by the gap formula which indicates $\Delta \propto L^{-1}$. The fitting of $\Delta(\infty)$ is 0.0332(3) at $J_y = 0.0$ and 0.943(1) at $J_y = 0.1$. If the amplification effect is considered, the real gap $\Delta(\infty)/\beta$ at $J_y = 0.0$ is

about 6.65×10^{-4} close to zero, which agrees well with the fact that the ES is gapless. These fitting results further prove our prediction that the ES gap has been magnified β times and explain why it looks so large at small J_y .